Descriptions of Useful Particle Physics Plots

GlueX-doc-4877

Curtis A. Meyer
Carnegie Mellon University

January 2021

Abstract

This document describes the different plots that are useful in GlueX analyses. The plots are based on the production of mesons and baryons, both of which may subsequently decay. The plots discussed are the Chew-Low plot, the Dalitz plot, and the Goldhaber plot. These used independently and together are useful to understand photoproduction reactions in GlueX.

1 Introduction

The goal of the GlueX Experiment [1] at Jefferson lab is to search for hybrid mesons using a linearly-polarized photon beam. Recent reviews on hybrid mesons [2, 3] provide an excellent description of the current experimental and theoretical situation. While not guaranteed to be true, it is in principle possible to produce all exotic hybridmesons in photoproduction [4].

In GlueX, we are looking at meson (M) and baryon (B) photoproduction reactions of the form

$$\vec{\gamma}p \quad \rightarrow \quad BM\,. \tag{1}$$

In many reactions, either the mesonic system M and/or the baryonic system B subsequently decay into two or more daughter particles. In this note, we will focus on the mesonic system where the final-state baryon is a proton. In these reactions, the amplitude analyses that are to be carried out in GlueX will look at the decay angular distributions of M, and that of its daughter particles. In an earlier note [5] we discussed the coordinate systems that are relevant for those analyses, in this note we will discuss several plots that are useful in carrying out these analyses. These include the Chew-Low plot [6], the Dalitz plot [7], and the Goldhaber plot [8, 9].

2 Kinematics

In this section we will look at the kinematics of reaction 2 where a photon of energy $\mathcal{E}_\gamma$ interacts with a proton target at rest, producing an out-going meson m and a recoil proton, p'. This is depicted in figure 1.

$$\gamma\, p \quad \rightarrow \quad p\, m \tag{2}$$

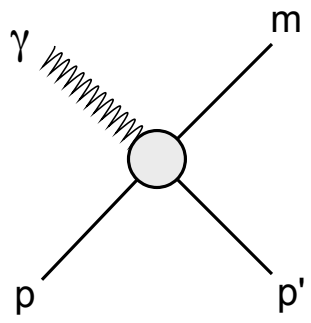

Figure 1: The scattering process for $\gamma\, p \rightarrow p\, m$.

2.1 The Mandelstam Variables

There are several Lorentz-invariant quantities that are relevant to the remainder of this note. Fore most are the Mandelstam variables [10], s, t and u which are computed from the four-momentum of the particles in the interaction. If we define p_γ and p_p to be the four-vectors of the incident

photon and the proton target, and p_m and p_b to be the four-momentum of the outgoing meson and baryon, then the Mandelstam variables are defined as

$$\begin{aligned} s &= (p_\gamma + p_p)^2 = (p_m + p_b)^2 && (3)\\ t &= (p_\gamma - p_m)^2 = (p_b - p_b)^2 && (4)\\ u &= (p_\gamma - p_b)^2 = (p_b - p_m)^2 \,. && (5) \end{aligned}$$

We also have the relation that

$$s + t + u = m_\gamma^2 c^4 + m_p^2 c^4 + m_m^2 c^4 + m_b^2 c^4 \,. \quad (6)$$

Four our photoproduction reactions, the Mandelstam variable s has a simple form

$$s = 2\,\mathcal{E}_\gamma\, m_p c^2 + (m_p c^2)^2 \,. \quad (7)$$

The total energy in the center of mass is represented by W which is

$$W = \sqrt{s} \,. \quad (8)$$

2.2 Lab versus Center of Mass Frames

Moving forward, the quantities p_γ, p_p, p_m and p_b will taken to be in the center of mass, while $\mathcal{E}_\gamma$ will represent the incident photon's energy in the GlueX lab frame. We will also note that the relativistic factors β and γ to move from the lab frame to the center of mass frame are

$$\begin{aligned} \beta &= \frac{\mathcal{E}_\gamma}{\mathcal{E}_\gamma + m_p c^2} && (9)\\ \gamma &= \frac{\mathcal{E}_\gamma + m_p c^2}{\sqrt{2\,\mathcal{E}_\gamma\, m_p c^2 + (m_p c^2)^2}} = \frac{\mathcal{E}_\gamma + m_p c^2}{\sqrt{s}} && (10)\\ \beta\gamma &= \frac{\mathcal{E}_\gamma}{\sqrt{s}} \,, && (11) \end{aligned}$$

where the relevant Lorentz boost is

$$p_{cm} = \begin{pmatrix} \gamma & 0 & 0 & -\beta\gamma \\ 0 & 1 & 0 & 0 \\ 0 & 0 & 1 & 0 \\ -\beta\gamma & 0 & 0 & \gamma \end{pmatrix} p_{lab} \,. \quad (12)$$

2.3 Center of Mass Momentum and Energy

It is also useful to know the magnitude of the three momentum q in the center of mass for the produced meson and baryon. These are both the same since $\vec{p}_b = -\vec{p}_m$. This can be expressed compactly in terms of the Källén function [11] or triangle function, defined in equation 13. The equivalent form in equation 14 tends to be more useful.

$$\begin{aligned} \lambda(x,y,z) &= x^2 + y^2 + z^2 - 2xy - 2xz - 2yz && (13)\\ \lambda(x,y,z) &= \left[x - (\sqrt{y} + \sqrt{z})^2\right]\left[x - (\sqrt{y} - \sqrt{z})^2\right] && (14) \end{aligned}$$

Using the Källén function, the magnitude of the three momentum q_m is given by

$$q_m^2 = \frac{\lambda(s, m_m^2c^4, m_b^2c^4)}{4s}, \tag{15}$$

which using equation 14, can be written as

$$q_m = \frac{\sqrt{[s-(m_mc^2+m_bc^2)^2]\ [s-(m_mc^2-m_bc^2)^2]}}{2\sqrt{s}}.$$

Similarly, the center-of-mass energy E_m of m is given as

$$E_m = \frac{1}{2\sqrt{s}}\left(s + m_m^2c^4 - m_b^2c^4\right), \tag{16}$$

and for the incident photon we have

$$E_\gamma = q_\gamma\, c = \frac{1}{2\sqrt{s}}\left(s - m_p^2c^4\right), \tag{17}$$

In the case of the meson subsequently decaying into two daughter particles, a and d, with masses m_a and m_d respectively, the magnitude of the three momentum q_a of both a and d in the rest frame of m is given by

$$q_a^2 = \frac{\lambda(m_m^2c^4, m_a^2c^4, m_d^2c^4)}{4m_a^2c^4}, \tag{18}$$

2.4 Limits on Mandelstam t

We can now look at the Mandelstam variable t.

$$\begin{aligned} t &= (p_\gamma - p_m)^2 \\ t &= m_m^2c^4 - 2p_\gamma \cdot p_m, \end{aligned}$$

We can evaluate the product of the two four vectors using the center-of-mass scattering angle θ as

$$\begin{aligned} p_\gamma \cdot p_m &= E_\gamma\, E_m - \vec{q}_\gamma \cdot \vec{q}_m c^2 \\ p_\gamma \cdot p_m &= E_\gamma\,(E_m - q_m c\cos\theta)\ . \end{aligned}$$

This yields the following unwieldy expression for t where we have explicitly taken the final state baryon to be a proton, $m_b = m_p$,

$$t = m_m^2c^4 - \frac{1}{2s}\left(s - m_p^2c^4\right)\left[\left(s + m_m^2c^4 - m_p^2c^4\right) - \lambda^{\frac{1}{2}}\left(s, m_m^2c^4, m_p^2c^4\right)\cos\theta\right]. \tag{19}$$

This can also be inverted to give $\cos\theta$ as a function of s, t and the masses.

$$\cos\theta = \frac{\left(s + m_m^2c^4 - m_p^2c^4\right) - 2s\ \left(t - m_m^2c^4\right) / \left(s - m_p^2c^4\right)}{\lambda^{\frac{1}{2}}\left(s, m_m^2c^4, m_p^2c^4\right)} \tag{20}$$

Noting that t will be less than or equal to zero, we can use equation 19, we can find the minimum and maximum values of $-t$. These occur at $\theta = 0$ and $\theta = \pi$ respectively.

$$(-t)_{min} = \frac{1}{2s}\left(s - m_p^2c^4\right)\left[\left(s + m_m^2c^4 - m_p^2c^4\right) - \lambda^{\frac{1}{2}}\left(s, m_m^2c^4, m_p^2c^4\right)\right] - m_m^2c^4 \quad (21)$$

$$(-t)_{max} = \frac{1}{2s}\left(s - m_p^2c^4\right)\left[\left(s + m_m^2c^4 - m_p^2c^4\right) + \lambda^{\frac{1}{2}}\left(s, m_m^2c^4, m_p^2c^4\right)\right] - m_m^2c^4 \quad (22)$$

Finally, by equation 6, for a fixed value of s, $\mid u \mid$ will be largest when $\mid t \mid$ is smallest and smallest when $\mid t \mid$ is largest. In the case of elastic scattering, $(-t)_{min} = 0$, which can be seen by setting $m_m = 0$ in our expression.

2.5 Invariant Masses

The final Lorentz invariant that we consider is the invariant mass. This is based on the relativistic energy-momentum relation

$$E^2 = (|\vec{p}|c)^2 + (mc^2)^2\,,$$

where m is the rest mass of the particle, which is a Lorentz invariant. This can be written as

$$(mc^2)^2 = E^2 - (|\vec{p}|c)^2$$

from which it is clear that the right-hand side is also Lorentz invariant, but that is just the square of the four momentum,

$$p \cdot p = E^2 - (|\vec{p}|c)^2\,,$$

so the square of the four momentum is a Lorentz invariant, which we define as the *invariant mass*. In our analyses, we have several particles that we are combining, and are interested in the invariant mass of the system. If we have two particles with four momentum p_1 and p_2, the the invariant mass of 1 and 2 is

$$m_{12}^2 = (p_1 + p_2)^2\,. \quad (23)$$

This can be extended to as many particles as we would like. For example, for $\omega \to \pi^+\pi^-\pi^0$, the mass of the ω is the invariant mass of the three *pi* system,

$$m_\omega^2 = (p_{\pi^+} + p_{\pi^-} + p_{\pi^0})^2\,. \quad (24)$$

3 Plots

3.1 The Chew-Low Plot

The Chew-Low was first presented by Geoffrey Chew and Francis Low in a paper on the analysis of scattering reactions with three or more particles in the final state [6]. For GlueX, this means we are considering variations of reaction 2 where the photo-produced meson m is unstable and decays into two or more daughter particles. For the two-body case, where the daughters are meson $\mathcal{M}_1$ and $\mathcal{M}_2$ with masses m_1 and m_2 respectively, the reaction in GlueX would be

$$\gamma p \to p\,\mathcal{M}_1\,\mathcal{M}_2 2\,,$$

where we then produce the invariant mass of the $\mathcal{M}_1$-$\mathcal{M}_2$ system as

$$m_m^2 c^4 \;=\; (p_1 + p_2)^2 \; .$$

The minimum value of m_m is

$$(m_m)_{min} c^2 \;=\; m_1 c^2 + m_2 c^2 \, , \tag{25}$$

and the maximum value is

$$(m_m)_{max} c^2 \;=\; W - m_p c^2 \, . \tag{26}$$

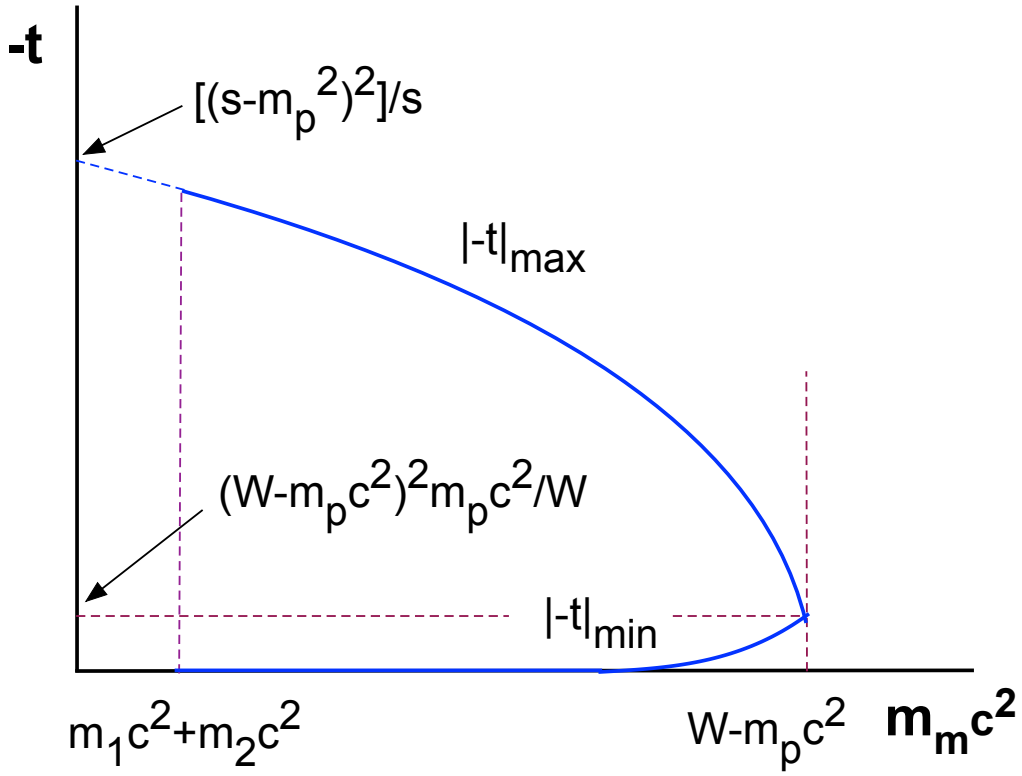

Figure 2: A Chew-Low plot where $-t$ is plotted against the invariant mass of the recoil meson system. The data occupy the region between the two horizontal dashed lines, and above the blue $|-t|_{min}$ and below the blue $|-t|_{max}$ curves.

In a Chew-Low plot, we plot $-t$ versus m_m as shown in Figure 2. The boundaries of the plot are described by equation 25 on the left, equation 26 on the right, equation 21 on the lower side and equation 22 on the upper side. Within those boundaries, meson resonances will appear as vertical

bands centered at the mass of the produced meson. The density will fall off with increasing $-t$ as the band goes up. The values of $|-t|_{min}$ and $|-t|_{max}$ have the same value of

$$|-t|_{min} \;=\; |-t|_{max} \;=\; (W - m_p c^2)\frac{m_p c^2}{W}$$

at $m_m c^2 = W - m_p c^2$. If there is u channel production, it will appear along the upper boundary of the plot. Because of both the rising value of $(-t)_{min}$ and the falling values of $(-t)_{max}$ as m_m increases, the relative production of high-mass meson states will be suppressed versus lower values.

3.2 The Dalitz Plot

A Dalitz plot [7] is used to analyze three-body final states. In our photoproduction reaction given in equation 2, the photo-produced meson m is unstable and decays into three daughter particles: $\mathcal{M}_1$, $\mathcal{M}_2$ and $\mathcal{M}_3$. These have masses m_1, m_2 and m_3 respectively. Unlike the Chew-Low plot, where the mass of the meson system m_m varies over a large range of values, a Dalitz plot is generally for a specific value of m_m, or a narrow range of masses. The reaction observed in GlueX would be

$$\gamma p \;\;\rightarrow\;\; pm \rightarrow p\,\mathcal{M}_1\,\mathcal{M}_2\,\mathcal{M}_3\,. \tag{27}$$

A more extensive description of Dalitz plots can be found in reference [12], but the following provides sufficient information on the plot. With a Dalitz plot, we are looking for intermediate resonances that contribute to reaction 27. We could have intermediate resonances that decay to any pair of mesons in the three-meson final state, as follows

$$\begin{aligned}
\gamma p \;&\rightarrow\; p\,\mathcal{M}_a\,\mathcal{M}_3 \;;\; \mathcal{M}_a \rightarrow \mathcal{M}_1\,\mathcal{M}_2 \\
\gamma p \;&\rightarrow\; p\,\mathcal{M}_b\,\mathcal{M}_2 \;;\; \mathcal{M}_b \rightarrow \mathcal{M}_1\,\mathcal{M}_3 \\
\gamma p \;&\rightarrow\; p\,\mathcal{M}_c\,\mathcal{M}_1 \;;\; \mathcal{M}_c \rightarrow \mathcal{M}_2\,\mathcal{M}_3\,.
\end{aligned}$$

For a Dalitz plot, we compute the pair-wise square of the invariant masses in the three-body system.

$$\begin{aligned}
m_{12}^2 c^4 &= (p_1 + p_2)^2 \\
m_{13}^2 c^4 &= (p_1 + p_3)^2 \\
m_{23}^2 c^4 &= (p_2 + p_3)^2
\end{aligned}$$

Given a particular meson mass, m_m, the three invariant masses are related by

$$m_m^2 \;=\; m_{12}^2 + m_{13}^2 + m_{23}^2 + m_1^2 + m_2^2 + m_3^2\,. \tag{28}$$

Thus, there are only two independent variable and the data can be represented by any pair of invariant masses. This leads to the Dalitz plot as shown in Figure 3, where one invariant mass squared is plotted against a second one. As noted in the plot, the third invariant mass squared actually follows a diagonal path coming in from the right. Resonances in $\mathcal{M}_1\mathcal{M}_2$ will appear as vertical bands, those in $\mathcal{M}_1\mathcal{M}_3$ will appear as horizontal bands, and those in $\mathcal{M}_2\mathcal{M}_3$ will appear as diagonal bands going from the lower right to the upper left. If m_m is taken as a range of values, rather than a single value, the diagonal bands will be washed out and may not be visible. Hence, it is often useful to produce the Dalitz plots in triplets, where the three possible pairs on on the vertical and horizontal axes.

It is also important to remember that a Dalitz plot shows invariant mass squared and not invariant mass. This is because the plot of masses squared would be uniformly populated if we had pur phase space distributions of events. Any deviation from flat or uniform distributions is associated with physics. That is not true when one plots mass. Finally, the density along bands in the Dalitz plot corresponds to the angular distribution of $\cos\theta_{helicity}$ for the decay of the two particles that form the band.

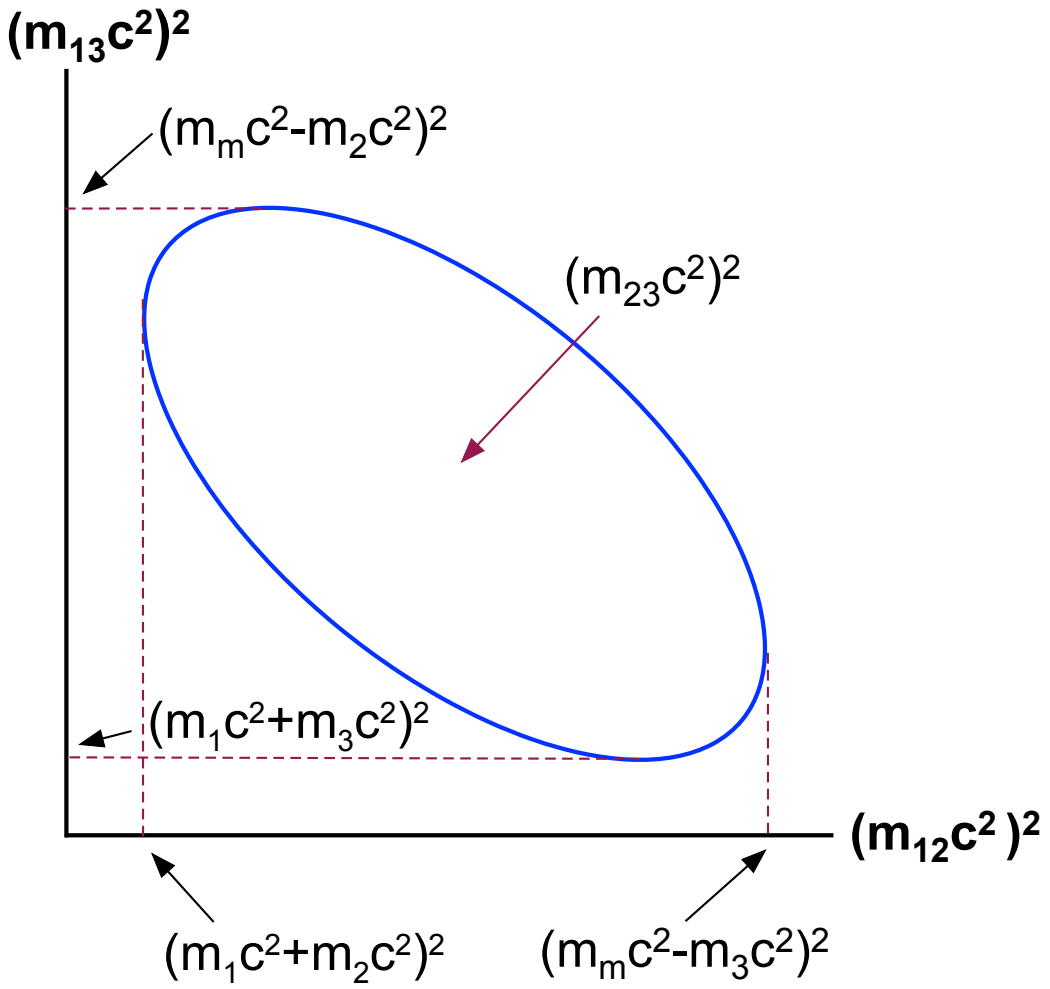

Figure 3: The Dalitz plot related to a system of energy m_m decaying to three daughter particles of masses m_1, m_2 and m_3. The Dalitz plot shows the invariant mass squared of one two-body subsystem, $m_{13}^2c^4$ plotted agains the invariant mass squared of a second pair, $m_{12}^2c^4$.

3.3 The Goldhaber Plot

A Goldhaber plot [8, 9] is used to analyze four (or more) body final states in scattering reactions like equation 2. An example of such a reaction is given in equation 27 where we have a proton and three mesons in the final state. The reaction is assumed to have center of mass energy W, where W can be a single value, or as in GlueX a range of values based on the incident photon energy. In the

case of the GlueX coherent peak going from $\mathcal{E}_\gamma = 8.4$ to 9 GeV. [1] For this range of beam energies, s varies from 16.64 to 17.77 GeV^2 and W has values between 4.08 and 4.22 GeV. Assuming the masses of the final state particles are m_1, m_2, m_3 and m_4, then the Goldhaber plot looks at the invariant mass of one two body system, $m_{34}c^2$ versus that of the other, $m_{12}c^2$, where each particle is used exactly once. Such a plot is shown in Figure 4. Hence, there are three possible Goldhaber

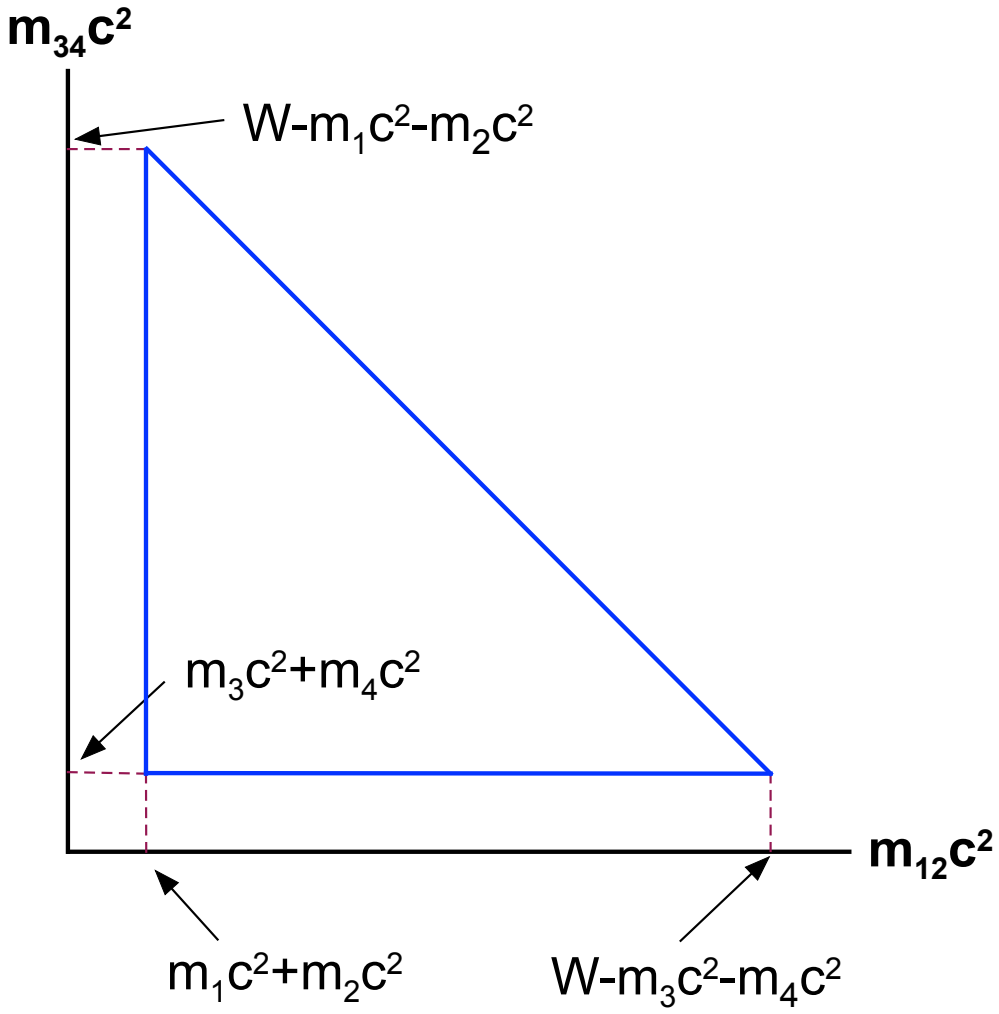

Figure 4: The Goldhaber plot looks at a scattering process where there are four final state particles of mass m_1, m_2, m_3 and m_4. The invariant mass of one pair, $m_{34}c^2$ is plotted against the other pair, $m_{12}c^2$, such that each particle only enters once.

plots that we can form for our four-body final state:

$$\begin{aligned} m_{34}c^2 \quad &\text{vs.} \quad m_{12}c^2 \\ m_{24}c^2 \quad &\text{vs.} \quad m_{13}c^2 \\ m_{23}c^2 \quad &\text{vs.} \quad m_{14}c^2 \,. \end{aligned}$$

[1] The 9 GeV edge in GlueX is based on a 12 GeV electron beam which we had once in late 2015. We hope to reach these design values in the future.

Unlike the Dalitz plot, phase space will not uniformly populate the plot of either mass or mss squared, so we just plot the masses on the two axes.

References

[1] S. Adhikari et. al. [GlueX Collaboration], **The GlueX Beamline and Detector**, Nucl. Instrum. & Meth. A**987**, 164807 (2021). DOI: 10.1016/j.nima.2020.164807.

[2] C. A. Meyer and Y. van Haarlem, **The Status of Exotic-quantum-number Mesons** Phys. Rev. C**82**, 025208 (2010). DOI: 10.1103/PhysRevC.82.025208.

[3] C. A. Meyer and E. S. Swanson, **Hybrid Mesons**, Progress in Particle and Nuclear Physics B**82**, 21, (2015). DOI: 10.1016/j.ppnp.2015.03.001

[4] C. A. Meyer, **The Production and Decay of Normal and Exotic-Hybrid Mesons in GlueX**, GlueX-Doc 4788 (2020).

[5] C. A. Meyer, **Coordinate Systems in GlueX**, GlueX-Doc 4829 (2021).

[6] G. F. Chew and F. E. Low, **Unstable Particles as Targets in Scattering Experiments**, Phys. Rev. **113**, 1640, (1959). DOI: 10.1103/PhysRev.113.1640

[7] R. H. Dalitz, **On the analysis of τ-meson data and the nature of the τ-meson**, Phil. Mag. Ser. 7, **44**, 1068 (1953). DOI: 10.1080/14786441008520365

[8] W. Chinowsky, G. Goldhaber, S. Goldhaber, W. Lee, T. O'Halloran, **On the Spin of the K^* Resonance**, Phys. Rev. Lett. 9, 330, (1962). DOI: 10.1103/PhysRevLett.9.330

[9] W. Chinowsky, G. Goldhaber, S. Goldhaber, W. Lee, T. O'Halloran, **Meson exchange in the reaction $K^+ + p \to K^* + N^*$**, Phys. Lett. **6**, 62 (1963) DOI: 10.1016/0031-9163(63)90222-1

[10] S. Mandelstam, **Determination of the Pion-Nucleon Scattering Amplitude from Dispersion Relations and Unitarity**, Phys. Rev. **112**, 1344 (1958). DOI: 10.1103/PhysRev.112.1344

[11] G. Källén, **Elementary Particle Physics**, (Addison-Wesley, 1964).

[12] C. A. Meyer, **General Properties Of Three-body Decays**, GlueX-Doc 3345 (2017).